Eur. Phys. J. C (2025) 85:830
https://doi.org/10.1140/epjc/s10052-025-14556-5

THE EUROPEAN PHYSICAL JOURNAL C

Regular Article - Theoretical Physics

Holographic spectroscopy of fermion with instantons

Si-wen Li[a], **Yi-peng Zhang**[b], **Hao-qian Li**[c]

Department of Physics, School of Science, Dalian Maritime University, Dalian 116026, China

Received: 8 April 2025 / Accepted: 18 July 2025

Abstract Using the gauge-gravity duality, we investigate the fermionic spectroscopy in the D(-1)-D3 brane system. The background geometry of this system described by IIB supergravity includes a black (deconfined) and bubble (confined) D3-brane which correspond respectively to a deconfined and a confined gauge theory in holography. The charge of the D(-1) brane as the D-instanton gives the gluon condensate in this model. To simplify the holographic setup, we first reduce briefly the ten-dimensional supergravity background produced by D(-1)-D3-branes to an equivalent five-dimensional background. Then the fermionic spectrum in the confined case is obtained by decomposing the fermion using dimensional reduction. In addition, by using the standard method for computing the Green's function in the AdS/CFT dictionary, we derive the equations for the fermionic correlation functions and solve them numerically with the infalling boundary condition. Our numerical results in the deconfined case illustrate that the fermionic correlation function as spectral function includes two branches of the dispersion curves whose behavior is very close to the results obtained from the method of hard thermal loop. And the effective mass generated by the medium effect of fermion splits into two values due to the spin-dependent interactions induced by instantons. In the confined case, the holographic correlation function indicates several separated dispersion curves which illustrates consistently the onset mass in the fermionic spectrum we obtained. Therefore, this work on holography demonstrates the instantonic configuration is very influential to the fermion in QCD.

[a] e-mail: siwenli@dlmu.edu.cn (corresponding author)
[b] e-mail: ypmahler111@dlmu.edu.cn
[c] e-mail: lihaoqian@dlmu.edu.cn

Contents

1 Introduction

In quantum chromodynamics (QCD), the instanton is known as the non-trivially topological excitation of the vacuum which contributes to the thermodynamics of QCD and relates to the breaking of chiral symmetry [1–3]. The instanton is also known to consist of constituents which are called BPS (Bogomol'nyi-Prasad-Sommerfield) monopoles or dyons [4], so there have been a lot of continuous researches to connect confinement and the breaking of chiral symmetry to the instanton constituents [5–13]. In particular, the dynamics of fermions involving instantons e.g. the spin-dependent interaction, fermionic quantum tunneling of the instantonic vacuum, is very interesting and widely discussed in the textbooks of QCD [1–3].

However, due to the property of asymptotic freedom, it is very challenging to investigate QCD in the low-energy region by using the perturbative method in quantum field theory (QFT) since QCD is strongly coupled in the low-energy region. Fortunately, the gauge-gravity duality provides an alternative way to study the strongly coupled QFT [14–16] using holography. In the top-down approach, the instanton is constructed simply as a geometric background with instantonic D-branes (D-instanton) [17–21], for example, the black D(-1)-D3 brane system can describe holographically the plasma with instantons in which the D(-1)-brane plays the role of instanton, and its dual field theory is the $\mathcal{N}=4$ super Yang–Mills theory with an instanton or a theta angle. So there have been many works based on the holographic instanton e.g. thermodynamics of Yang–Mills theory [22], hadronic spectrum [23,24], real-time dynamics [25], Chern–Simons theory [26,27], chiral symmetry breaking [28], quark potential [29–31], Schwinger effect [32–34], the hadronic interaction [35]. Despite all this, the study of fermions in the presence of the instanton remains unexplored in the existing works in holography although it attracts great interests as it is reviewed in [1–3] in QFT. Therefore, the goal of this work is to explore the dynamics of fermions in the presence of an instanton as a starting point for further investigations, since it can be evaluated by using the most fundamental principle in holography.

For our goal, the setup in this work starts with the D(-1)-D3 brane system since it describes simply the instantons in gauge theory through gauge-gravity duality [17,25,28]. Then, we reduce the 10d IIB supergravity background produced by black D3-branes with D(-1)-branes to an effective five-dimensional (5d) geometric background. We note that the supergravity solution for the D(-1)-D3 brane system includes a black (deconfined) and a bubble (confined) D3-brane solution which corresponds respectively to a deconfined and a confined gauge theories with instantons in holography [36,37]. Afterwards, we study a probe bulk fermion in the 5d geometric background and derive its covariant Dirac equation. In the confined geometry, we decompose the bulk fermion using dimensional reduction, evaluate numerically the holographic spectrum of fermion. Since the bulk fermion must be a gauge-invariant operator, we identify it with a baryon in field theory.[1] In addition, we investigate the fermionic two-point correlation function in the dual theory by employing the standard technique in the AdS/CFT dictionary so that obtain the differential equations for the fermionic correlators in the bulk.[2] By imposing the infalling boundary condition at the horizon, we afterwards solve the fermionic correlation functions numerically both in deconfined and confined backgrounds. Our numerical calculation in the deconfined case illustrates that, without the D-instanton, there is only one branch of the holographic dispersion curves for fermion lying on the light-cone which is similar as the existing works about holographic fermions [35,42,46–49]. In the presence of the D-instanton, the fermionic correlation function has a correction which to leading order splits the dispersion curves into two branches at small momentum, and this behavior is very close to the dispersion curves from the approach of hard thermal loop (HTL) in QFT. Furthermore, the two branches of the dispersion curves reveals that the effective bound mass of fermion in plasma has two values in the presence of the D-instanton. Remarkably it agrees qualitatively with effective potential for the spin-dependent interactions induced by instantons computed by the process of one-gluon exchange in QCD [1,2]. In the confined case, the holographic correlation function indicates several separated dispersion curves which agrees with the fermionic spectrum we obtained. Therefore, this work, as a starting point, is a holographic reproduction of the properties of fermions in the presence of instantons, we believe the instantonic configuration in QCD is very influential to the fermion.

The outline of this manuscript is as follows. In Sect. 2, we collect the essentials of the 10d supergravity background produced by D3-branes with D(-1)-branes as D-instantons, and reduce it briefly to an effectively 5d gravity background. In Sect. 3, we decompose the bulk spinor with dimensional reduction, then evaluate the eigenmass of fermion numerically. In Sect. 4, we demonstrate the principle in AdS/CFT dictionary to compute the holographic correlation function for spinor. Then we derive the covariant Dirac equation and the holographic counter term for spinor in order to obtain the differential equations for the fermionic correlators. In Sect. 4, we solve numerically the holographic fermionic correlation functions order by order with physical analysis and interpretation, both in the deconfined and confined case. The final section is the summary.

Notation

In this manuscript, the capital letters L, M, N... refer to the indices of the bulk coordinate as x^M, the lowercase letters a, b, c refer to the corresponding indices of the coordinate in tangent space. The gamma matrices γ^a, Γ^M as the generators of the Clifford algebra with vielbein e^a_M are related as,

$$\left\{\gamma^a, \gamma^b\right\} = 2\eta^{ab}, \left\{\Gamma^M, \Gamma^M\right\} = 2g^{MN},$$
$$\Gamma^M = e^M_a\gamma^a, g_{MN} = e^a_M\eta_{ab}e^a_N, \tag{1.1}$$

where g_{MN} refers to the metric on a manifold and η_{ab} refers to the Minkowskian metric. The spin connection ω_{Mab} is

[1] Since baryon is the fermionic gauge-invariant operator in QCD, for a bottom-up or phenomenological approach of QCD, the fermionic gauge-invariant operator is usually identified to a baryon, e.g. [38]. The top-down approaches also support that the gauge-invariant fermions behave as baryons as it is discussed in [39,40]. In particular, baryon can be introduced into the holographic approaches by considering the baryon vertex as it is discussed in [41] and the relevant works with baryon vertex can also be reviewed in [35,42,43].

[2] The two-point functions of fermions in the context of the AdS/CFT were first considered in [44,45].

defined as,

$$\omega_{Mab} = \eta_{cb}\left(e_a^N \partial_M e_N^c - e_a^N \Gamma_{MN}^K e_K^c\right), \tag{1.2}$$

where the affine connection Γ_{MN}^K is given by,

$$\Gamma_{MN}^K = g^{KL}\left(\partial_M g_{LN} + \partial_N g_{ML} - \partial_L g_{MN}\right). \tag{1.3}$$

The Greek letters as μ, ν...refer to the indices of coordinate as x^μ at the holographic boundary. The lowercase letters i, j, k, l run over the spatial directions of the holographic boundary i.e. $i, j, k, l = 1, 2, 3$. The gamma matrices presented in this work are chosen as $\gamma^a = \{\gamma^\mu, \gamma\}$ as,

$$\gamma^\mu = i\begin{pmatrix} 0 & \sigma^\mu \\ \bar{\sigma}^\mu & 0 \end{pmatrix}, \gamma = \begin{pmatrix} 1 & 0 \\ 0 & -1 \end{pmatrix}, \tag{1.4}$$

with $\sigma^\mu = \left(1, -\sigma^i\right), \bar{\sigma}^\mu = \left(1, \sigma^i\right), i = 1, 2, 3$, where σ^i s are the Pauli matrices.

2 The instantonic background in holography

In this section, let us briefly review the instantonic background which corresponds to the system consisting of N_c D3-branes with N_{D} D-instantons i.e. the D(-1)-branes in the large-N_c limit in the type IIB string theory [17,18,25]. Then, we integrate out the S^5 part in order to obtain a five-dimensional (5d) background geometry for simplification.

2.1 The D3-brane background with D-instanton

The supergravity solution of N_c D3-branes with N_{D} D-instantons is in general described by a 10d deformed D3-brane solution with a non-trivial Ramond-Ramond (R-R) zero form C_0. It is recognized as a marginal "bound state" of D3-branes with smeared N_{D} D(-1)-branes. In our notation, N_c D3-branes are identified as color branes, hence the associated number N_c denotes the color number. In the large-N_c limit, the 10d bosonic type IIB supergravity action describes the low-energy dynamics of this system which is given in the string frame as,

$$S_{\mathrm{IIB}} = \frac{1}{2\kappa_{10}^2}\int d^{10}x\sqrt{-g}\left[e^{-2\Phi}\left(\mathcal{R} + 4\partial\Phi\cdot\partial\Phi\right) - \frac{1}{2}\left|F_1\right|^2 - \frac{1}{2}\left|F_5\right|^2\right], \tag{2.1}$$

where $2\kappa_{10}^2 = (2\pi)^7 l_s^8$ is the 10d gravity coupling constant, l_s, g_s is respectively the string length and the string coupling constant. We use Φ to denote the dilaton field and $F_{1,5}$ is the field strength of the R-R zero and four form $C_{0,4}$ respectively. The solution of N_c D3-branes with N_{D} D-instantons is the near-horizon solution of non-extremal D3-branes with a non-trivial C_0, which in string frame reads [17,18,25],

$$\begin{aligned} ds^2 &= e^{\frac{\phi}{2}}\left\{\frac{r^2}{R^2}\left[-f(r)\,dt^2 + d\mathbf{x}\cdot d\mathbf{x}\right] + \frac{1}{f(r)}\frac{R^2}{r^2}dr^2 + R^2 d\Omega_5^2\right\}, \\ e^\phi &= 1 + \frac{Q}{r_H^4}\ln\frac{1}{f(r)},\ f(r) = 1 - \frac{r_H^4}{r^4}, \\ F_5 &= dC_4 = g_s^{-1}\mathcal{Q}_3\epsilon_5, \\ F_1 &= dC_0,\ C_0 = -ie^{-\phi} + i\mathcal{C},\ \phi = \Phi - \Phi_0,\ e^{\Phi_0} = g_s, \end{aligned} \tag{2.2}$$

where $\mathcal{C}$ is a boundary constant for C_0, ϵ_5 is the volume element of a unit S^5. And the associated parameters are given as,

$$R^4 = 4\pi g_s N_c l_s^4,\ \mathcal{Q}_3 = 4R^4,\ Q = \frac{N_{\mathrm{D}}}{N_c}\frac{(2\pi)^4\alpha'^2}{V_4}\mathcal{Q}_3. \tag{2.3}$$

Here, $x^\mu = \{t, \mathbf{x}\} = \left\{t, x^i\right\},\ i = 1, 2, 3$ refers to the 4d spacetime where the D3-branes are extended along. And r is the holographic direction perpendicular to the D3-branes. The solution (2.2) is asymptotically $\mathrm{AdS}_5 \times S^5$ at the holographic boundary $r \to \infty$ which describes geometrically that the D-instanton charge N_{D} is smeared over the worldvolume V_4 of the N_c coincident black D3-branes homogeneously with a horizon at $r = r_H$.[3] The backreaction of the D-instantons has been taken into account in the background, thus it implies N_{D}/N_c must be fixed in the large-N_c limit. The dual theory of this background is conjectured to be the 4d $\mathcal{N} = 4$ super Yang–Mills theory (SYM) in a self-dual gauge field (instantonic) background or with a dynamical axion at finite temperature characterized by the parameter Q [17,18]. Note that, in the language of hadron physics, C_0 is recognized as the axion. The gluon condensate in this system can be evaluated as,

$$\left\langle \mathrm{Tr} F_{\mu\nu}F^{\mu\nu}\right\rangle \simeq \frac{N_{\mathrm{D}}}{16\pi^2 V_4} = \frac{1}{16}\frac{Q}{(2\pi\alpha')^2 R^4}\frac{N_c}{(2\pi)^4},\quad \mu, \nu = 0, 1...3. \tag{2.4}$$

Besides, by following [36,50], there is a confining background which can be obtained from (2.2). That is to compactify one of the spatial dimension $x^3 = y$ of the D3-brane on a circle S^1, so the worldvolume theory on the D3-branes is effectively 3d below the energy scale $M_{KK} = \frac{2\pi}{\delta y}$, where δy refers to the size of S^1. Then identify the bulk supergravity geometry that has this geometry for its boundary, which resultantly leads to a double Wick rotation ($t \to -iy,\ y \to -it$)

[3] When the IR cut-off is taken into account, V_4 can be chosen to be finite [17].

on the background presented in (2.2) as,

$$ds^2 = e^{\frac{\phi}{2}} \left\{ \frac{r^2}{R^2} \left[\eta_{\mu\nu} dx^\mu dx^\nu + f(r) dy^2 \right] + \frac{1}{f(r)} \frac{R^2}{r^2} dr^2 + R^2 d\Omega_5^2 \right\}, \mu, \nu = 0, 1, 2.$$
$$f(r) = 1 - \frac{r_{KK}^4}{r^4}. \tag{2.5}$$

The background (2.5) is defined only for $r > r_{KK}$ and it does not have a horizon, so r_{KK} is the end of the spacetime. Since the warp factor $e^{\frac{\phi}{2}} \frac{r^2}{R^2}$ never goes to zero, the Wilson loop asymptotics lead to an area law which manifests as confinement in the dual theory.

2.2 The effective 5d background

The S^5 part in the gravity solution (2.1) and (2.2) can be integrated out so that the background (2.2) can reduce to an equivalent 5d background. Since all the fields presented in (2.1) and (2.2) are expected to depend on the coordinates x^μ, r only, it is possible to integrate out the S^5 part in action with

$$ds^2_{(10\text{d})} = ds^2_{(5\text{d})} + ds^2_{S^5}. \tag{2.6}$$

So in the Einstein frame, the action (2.1) becomes,

$$S_{\text{IIB}}^{(5\text{d})} = \frac{1}{2\kappa_5^2} \int d^5x \sqrt{-g^{(5\text{d})}} \left[\mathcal{R}^{5\text{d}} - \frac{1}{2} \partial\Phi \cdot \partial\Phi - \frac{1}{2} |dC_0|^2 - 2\Lambda \right], \tag{2.7}$$

where the cosmological constant Λ is obtained by

$$\Lambda = \frac{(2\pi l_s)^5}{2} \int_{S^5} dx^5 \sqrt{-g_{S^5}} |F_5|^2 = -\frac{6}{R^2}. \tag{2.8}$$

Since the supergravity solution (2.2) implies that the kinetic terms of Φ, C_0 presented in (2.7) cancel each other, the 5d solution is nothing but AdS$_5$. Thus, in the string frame it is given as,

$$ds^2_{(5\text{d})} = e^{\frac{\phi}{2}} \left\{ \frac{r^2}{R^2} \left[-f(r) dt^2 + d\mathbf{x} \cdot d\mathbf{x} \right] + \frac{1}{f(r)} \frac{R^2}{r^2} dr^2 \right\}, \tag{2.9}$$

and the solution for Φ and C_0 are still given by the corresponding formulas given in (2.2). Note that the action (2.7) describes nothing but the gravity-dilaton-axion system, and we will use the 5d effective background (2.9) in z coordinate as,

$$ds^2_{(5\text{d})} = e^{\frac{\phi}{2}} \frac{R^2}{z^2} \left[-f(z) dt^2 + d\mathbf{x} \cdot d\mathbf{x} + \frac{dz^2}{f(z)} \right],$$
$$f(z) = 1 - \frac{z^4}{z_H^4}, e^\phi = 1 - q \ln f(z),$$
$$z = \frac{R^2}{r}, z_H = \frac{R^2}{r_H}, q = \frac{z_H^4 Q}{R^8}. \tag{2.10}$$

in which the holographic boundary is located at $z \to 0$ to continue our discussion. Moreover, the confined geometry presented (2.5) also reduces to an effective 5d background as,

$$ds^2_{(5\text{d})} = e^{\frac{\phi}{2}} \frac{R^2}{z^2} \left[\eta_{\mu\nu} dx^\mu dx^\nu + f(r) dy^2 + \frac{dz^2}{f(z)} \right],$$
$$f(z) = 1 - \frac{z^4}{z_{KK}^4}, e^\phi = 1 - q \ln f(z),$$
$$z = \frac{R^2}{r}, z_H = \frac{R^2}{r_{KK}}, q = \frac{z_{KK}^4 Q}{R^8}. \tag{2.11}$$

3 The spectrum of the baryonic fermion

In this section, our concern is the fermionic spectrum in the confined geometry. As the Wilson loop asymptotics lead to an area law, we consider a fermionic operator in the boundary theory which describes a confined state. In particular, the fermionic operator should be gauge-invariant according to gauge-gravity duality[4] [15,16,36]. As the confined metric given in (2.11) becomes 3d below the energy scale M_{KK}, it reduces to the following metric,

$$ds^2_{(4\text{d})} = e^{\frac{\phi}{2}} \frac{R^2}{z^2} \left[\eta_{\mu\nu} dx^\mu dx^\nu + \frac{dz^2}{f(z)} \right],$$
$$\equiv g_{xx} \eta_{\mu\nu} dx^\mu dx^\nu + g_{zz} dz^2. \tag{3.1}$$

We start with a bulk fermion ψ as the dual mode to the baryonic fermion at the boundary propagating on the background (3.1). Its Dirac action is given as,

$$S_{\text{bulk}} = i \int d^4x \sqrt{-g} \bar{\psi} \left(\Gamma^M \nabla_M - m \right) \psi, \tag{3.2}$$

where the Dirac operator is computed as,

$$\Gamma^M \nabla_M = \frac{1}{\sqrt{g_{xx}}} \gamma^\mu \partial_\mu + \frac{1}{\sqrt{g_{zz}}} \gamma \partial_z + \frac{3}{4} \frac{\partial_z \ln g_{xx}}{\sqrt{g_{zz}}} \gamma. \tag{3.3}$$

[4] The gauge-invariant fermion in the confined phase of QCD is a baryon. In the top-down approach, it can be constructed by introducing a baryon vertex [35,42,43]. However, since we are following a bottom-up approach, we will not attempt to discuss the holographic construction of a baryon with a baryon vertex in this work.

So the Dirac equation (3.2) can be rewritten as,

$$S_{\text{bulk}} = i \int d^3xdz\bar{\psi}\left(A_1\gamma^\mu\partial_\mu + A_2\gamma\partial_z + A_3\gamma + A_4\right)\psi, \tag{3.4}$$

where the coefficients are

$$A_1 = \sqrt{-\frac{g}{g_{xx}}}, A_2 = \sqrt{-\frac{g}{g_{zz}}},$$
$$A_3 = \frac{3}{4}\partial_z \ln g_{xx}\sqrt{-\frac{g}{g_{zz}}}, A_4 = m\sqrt{-g}. \tag{3.5}$$

Let us further decompose the spinor ψ as a series of the basis function as,

$$\psi = \sum_{n,k}\begin{pmatrix}\psi_+^{(n)}F_+^{(n)}\\ \psi_-^{(k)}F_-^{(k)}\end{pmatrix}, \tag{3.6}$$

where $\psi_\pm^{(k)}$ depends on x^μ and $F_\pm^{(k)}$ depends on z. Then, we insert the decomposition in the action (3.4), and it becomes

$$\begin{aligned}S_{\text{bulk}} = &-\sum_{k,n}\int d^3xdz\Big[\psi_-^{(k)\dagger}F_-^{(k)}A_2\psi_+^{(n)}\partial_zF_+^{(n)}\\ &+\psi_-^{(k)\dagger}F_-^{(k)}A_3\psi_+^{(n)}F_+^{(n)}\\ &+\psi_-^{(k)\dagger}F_-^{(k)}A_4\psi_+^{(n)}F_+^{(n)}+\psi_-^{(k)\dagger}F_-^{(k)}A_1i\sigma^\mu\partial_\mu\psi_-^{(n)}F_-^{(n)}\\ &+\psi_+^{(n)\dagger}F_+^{(n)}A_1i\bar{\sigma}^\mu\partial_\mu\psi_+^{(k)}F_+^{(k)}-\psi_+^{(n)\dagger}F_+^{(n)}A_2\psi_-^{(k)}\partial_zF_-^{(k)}\\ &-\psi_+^{(n)\dagger}F_+^{(n)}A_3\psi_-^{(k)}F_-^{(k)}+\psi_+^{(n)\dagger}F_+^{(n)}A_4\psi_-^{(k)}F_-^{(k)}\Big].\end{aligned} \tag{3.7}$$

By imposing the normalization condition for the basis function,

$$\int dzF_+^{(k)}F_+^{(n)} = \int dzF_-^{(k)}F_-^{(n)} = \delta^{kn}, \tag{3.8}$$

with eigenequations

$$\begin{aligned}&\frac{A_2}{\sqrt{A_1}}\partial_z\left(\frac{F_-^{(n)}}{\sqrt{A_1}}\right)+\frac{A_3-A_4}{A_1}F_-^{(n)} = -M_nF_+^{(n)},\\ &\frac{A_2}{\sqrt{A_1}}\partial_z\left(\frac{F_+^{(n)}}{\sqrt{A_1}}\right)+\frac{A_3+A_4}{A_1}F_+^{(n)} = M_nF_-^{(n)},\end{aligned} \tag{3.9}$$

action (3.7) reduces to the standard form of kinetic term for fermion as,

$$\begin{aligned}S = &-\sum_n\int d^3x\Big\{\psi_-^{(n)\dagger}i\sigma^\mu\partial_\mu\psi_-^{(n)}+\psi_+^{(n)\dagger}i\bar{\sigma}^\mu\partial_\mu\psi_+^{(n)}\\ &+M_n\left[\psi_-^{(n)\dagger}\psi_+^{(n)}+\psi_+^{(n)\dagger}\psi_-^{(n)}\right]\Big\}.\end{aligned} \tag{3.10}$$

Table 1 The fermionic spectrum with $m = 0$ in the unit of $M_{KK} = 1$

$q = 0$	$n = 1$	$n = 2$	$n = 3$	$n = 4$
M_+	1.7899	4.2721	6.7597	9.2568
M_-	1.8131	4.2978	6.7868	9.2853

The eigenvalue M_n can be evaluated by solving numerically the following eigenequations

$$\begin{aligned}&\frac{A_2}{\sqrt{A_1}}\partial_z\left(\frac{A_2}{A_1}\partial_z\left(\frac{F_+^{(n)}}{\sqrt{A_1}}\right)+\frac{A_3+A_4}{A_1}F_+^{(n)}\right)\\ &\quad+\frac{A_3-A_4}{A_1}\left(\frac{A_2}{\sqrt{A_1}}\partial_z\left(\frac{F_+^{(n)}}{\sqrt{A_1}}\right)+\frac{A_3+A_4}{A_1}F_+^{(n)}\right)\\ &= -M_n^2F_+^{(n)},\\ &\frac{A_2}{\sqrt{A_1}}\partial_z\left(\frac{A_2}{A_1}\partial_z\left(\frac{F_-^{(n)}}{\sqrt{A_1}}\right)+\frac{A_3-A_4}{A_1}F_-^{(n)}\right)\\ &\quad+\frac{A_3+A_4}{A_1}\left(\frac{A_2}{\sqrt{A_1}}\partial_z\left(\frac{F_-^{(n)}}{\sqrt{A_1}}\right)+\frac{A_3-A_4}{A_1}F_-^{(n)}\right)\\ &= -M_n^2F_-^{(n)}.\end{aligned} \tag{3.11}$$

We note that, the mass m presented in (3.2) is the only parameter to fit the experimental data. For massless fermion $m = 0$, the equations for $F_\pm^{(n)}$ are identical. For $m \neq 0$, the mass spectrum of $M_n^\pm$ is separated with the separation $\sim m/2$. According to (3.6), the "±" can be identified to the proper quantum numbers of a baryon e.g. the 3rd component of the isospin. In this sense, we solve (3.11) with sufficiently small mass parameter $m = 0.01$ and the associated mass spectrum is given in Table 1 and its dependence on q is illustrated in Fig. 1. The numerical results are related the fact that the mass of baryons as the up and down components of a isospin is roughly equal. The mass spectrum is less dependent on the instanton density. However the separation of the eigenmass does not match very well to the experimental data for the lowest baryon mass. For example, if we identify the states of mass $M_1^\pm$, $M_2^\pm$ as proton ($n = 1, I = +1/2$), neutron ($n = 1, I = -1/2$), Σ^+ ($n = 1, I = +1/2$), Σ^- ($n = 1, I = -1/2$), the mass ratio of Σ^+ and proton given in this model is $M_2^+/M_1^+ \simeq 2.39$ less close to the experimental data $M_{\text{proton}}/M_{\Sigma^+} \simeq 1.27$. One possible reason may be that the current theory is 3d instead of a 4d theory.

4 The fermionic correlation function

In this section, we focus on the fermionic correlation function as a parallel method to investigate the fermionic spectrum. By introducing a probe fermion in the bulk geometry,

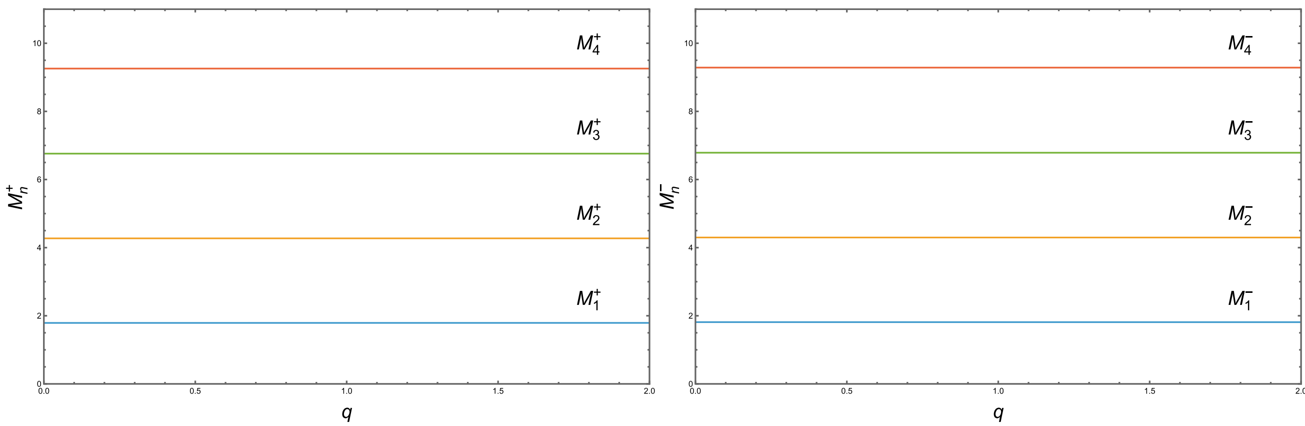

Fig. 1 The mass spectrum as a function of the instanton density q

we will evaluate its two-point Green function in holography by employing the standard method in the AdS/CFT dictionary. Since the fermion must be a gauge-invariant operator, it could be a baryonic fermion. In particular, the influence of the instanton charge denoted by q in the fermionic correlation function is also considered.

4.1 General setup for the fermionic correlation function

Let us start with the principle of the AdS/CFT which postulates that the generating functional of the dual conformal field theory (CFT) $Z_{\rm CFT}$ is equal to its gravitational partition function $Z_{\rm gravity}$ in the bulk geometry. Namely, for a spinor field ψ in the $D+1$ dimensional bulk, we have [44,45,51]

$$Z_{\rm CFT}\left[\bar{\psi}_0, \psi_0\right] = Z_{\rm gravity}\left[\bar{\psi}, \psi\right]|_{\bar{\psi},\psi\to\bar{\psi}_0,\psi_0}, \tag{4.1}$$

with

$$\begin{aligned} Z_{\rm CFT}\left[\bar{\psi}_0, \psi_0\right] &= \left\langle \exp\left\{\int_{\partial\mathcal{M}} \left(\bar{\eta}\psi_0 + \bar{\psi}_0\eta\right) d^D x\right\}\right\rangle, \\ Z_{\rm gravity}\left[\bar{\psi}, \psi\right] &= e^{-S^{ren}_{\rm gravity}}, \\ S^{ren}_{\rm gravity} &= \int_{\mathcal{M}} \mathcal{L}^{ren}_{\rm gravity}\left[\bar{\psi}, \psi\right]\sqrt{-g}d^{D+1}x \end{aligned} \tag{4.2}$$

Note that, we use $\mathcal{M}$ to denote the bulk space and its holographic boundary is given at $\partial\mathcal{M} = \{z \to 0\}$. ψ_0 refers to the boundary value of ψ as a source of the boundary fermionic operator η. Since ψ, η are fermionic gauge-invariant operator, η is expected to be a baryon or a baryonic plasmino phenomenologically in this work. $\mathcal{L}^{ren}_{\rm gravity}$ denotes the renormalized Lagrangian of the bulk field ψ. Then following the standard steps in quantum field theory (QFT), the one-point function i.e. average value of $\bar{\eta}$ is given as

$$\langle\bar{\eta}\rangle = \frac{1}{Z_{\rm CFT}}\frac{\delta Z_{\rm CFT}}{\delta\psi_0} = \frac{1}{Z_{\rm gravity}}\frac{\delta Z_{\rm gravity}}{\delta\psi_0} = -\frac{\delta S^{ren}_{\rm gravity}}{\delta\psi_0} \equiv \Pi_0, \tag{4.3}$$

where we have used the relation (4.1). Therefore, the two-point correlation function G_R of η is obtained as,

$$\left\langle\bar{\eta}\left(\omega, \vec{k}\right)\right\rangle = G_R\left(\omega, \vec{k}\right)\psi_0, \tag{4.4}$$

i.e.

$$\Pi_0 = G_R\left(\omega, \vec{k}\right)\psi_0, \tag{4.5}$$

where $\omega, \vec{k}$ refers to the frequency and 3-momentum of the associated Fourier modes. Altogether, it is possible to evaluate ψ_0, Π_0 in order to evaluate the two-point correlation function G_R of η by using the classical gravity action $S^{ren}_{\rm gravity}$ in holography.

4.2 Covariant Dirac equation for a probe fermion

Keep the formulas in Sect. 4.1 in hand, let us investigate a probe fermion in the D+1-dimensional holographic background (2.10). In general, the D+1-dimensional homogeneous background metric can be written as,

$$ds^2_{(5d)} = g_{tt}dt^2 + g_{xx}d\mathbf{x}\cdot d\mathbf{x} + g_{zz}dz^2, \tag{4.6}$$

where g_{tt}, g_{xx}, g_{zz} depend on z only. For a probe fermion in bulk, its dynamic is described by the Dirac action given in (3.2), so the Dirac equation reads

$$\left(\Gamma^M\nabla_M - m\right)\psi = 0, \tag{4.7}$$

where the covariant derivative operator is given in terms of the spin connection as,

$$\nabla_M = \partial_M + \frac{1}{4}\omega_{Mab}\gamma^{ab}, \gamma^{ab} = \frac{1}{2}\left[\gamma^a, \gamma^b\right]. \tag{4.8}$$

Imposing the homogeneous metric (4.6), the Dirac operator is computed as,

$$\Gamma^M \nabla_M = \frac{1}{\sqrt{-g_{tt}}}\gamma^0\partial_0 + \frac{1}{\sqrt{g_{xx}}}\gamma^i\partial_i + \frac{1}{\sqrt{g_{zz}}}\gamma\partial_z + \frac{1}{4g_{xx}g_{tt}\sqrt{g_{zz}}}\left[(D-1)\,g_{tt}g'_{xx} + g_{xx}g'_{tt}\right]\gamma. \tag{4.9}$$

To find a solution for the Dirac equation, we insert the ansatz for spinor ψ in Dirac representation as,

$$\psi = \begin{pmatrix}\psi_R\\ \psi_L\end{pmatrix} = \left(-gg^{zz}\right)^{-1/4}\int \frac{d^4p}{(2\pi)^4}e^{ik\cdot x}\chi(z,k),$$
$$\chi(z,k) = \begin{bmatrix}\chi_R(z,k)\\ \chi_L(z,k)\end{bmatrix}, \chi_{R,L} = \begin{pmatrix}\chi^{(1)}_{R,L}\\ \chi^{(2)}_{R,L}\end{pmatrix}, k_\mu = (k_0, k_i), \tag{4.10}$$

into the Dirac equation (4.7), so it is simplified as,

$$\left[\sqrt{\frac{g_{xx}}{g_{zz}}}\left(\gamma\partial_z - m\sqrt{g_{zz}}\right) + iK_\mu\gamma^\mu\right]\chi(z,k) = 0, \tag{4.11}$$

where

$$K_\mu = \left(\sqrt{-\frac{g_{xx}}{g_{tt}}}k_0, k_i\right). \tag{4.12}$$

4.3 Construction for the correlation function

When the background metric (4.6) is inserted into (4.11), the Dirac equation reduces to two decoupled differential equations for $\chi_{R,L}$ as,

$$\left(\partial_z + m\sqrt{g_{zz}}\right)\left[(K\cdot\sigma)^{-1}\sqrt{\frac{g_{xx}}{g_{zz}}}\left(\partial_z - m\sqrt{g_{zz}}\right)\chi_R\right] = -\sqrt{\frac{g_{zz}}{g_{xx}}}\left(K\cdot\bar{\sigma}\right)\chi_R,$$
$$\left(\partial_z - m\sqrt{g_{zz}}\right)\left[(K\cdot\bar{\sigma})^{-1}\sqrt{\frac{g_{xx}}{g_{zz}}}\left(\partial_z + m\sqrt{g_{zz}}\right)\chi_L\right] = -\sqrt{\frac{g_{zz}}{g_{xx}}}\left(K\cdot\sigma\right)\chi_L, \tag{4.13}$$

which can be solved analytically near the boundary $z \to 0$ as,

$$\chi_R = Cz^{1-mR} + Dz^{mR},$$
$$\chi_L = Az^{-mR} + Bz^{1+mR}. \tag{4.14}$$

where A, B, C, D are constant Weyl spinor depending on 4-momentum k and the charge of the D-instanton q. Hence for $mR > 0$, the boundary value χ_0 of χ is given by A which is the most divergent term, defined as

$$\chi_0 = \lim_{z\to 0} z^{mR}\chi = \begin{pmatrix}0\\ A\end{pmatrix}. \tag{4.15}$$

Then recall the Dirac action (3.2) with (4.10), it leads to

$$S_{\text{bulk}} = i\int d^4xdz\sqrt{-g}\bar{\psi}\left(\Gamma^M\nabla_M - m\right)\psi$$
$$= i\int d^4x\left(\bar{\chi}\gamma\chi\right)|^0_{z_H} - i\int d^4xdz\sqrt{\frac{g_{zz}}{g_{xx}}}\left[\sqrt{\frac{g_{xx}}{g_{zz}}}\left(\partial_z\bar{\chi}\gamma + m\sqrt{g_{zz}}\bar{\chi}\right) + iK_\mu\bar{\chi}\gamma^\mu\right]\chi. \tag{4.16}$$

Note that the last term in (4.16) vanishes since it is nothing but the conjugate equation of (4.11). Therefore, we can obtain a boundary action S_{bdry} from (4.16) as,

$$S_{\text{bdry}} = i\int d^4x\left(\bar{\chi}\gamma\chi\right)|_{z\to 0}$$
$$= i\int d^4x\left(D^\dagger A + C^\dagger Az^{1-2m}\right)|_{z\to 0}, \tag{4.17}$$

which implies the holographic counterterm S_{CT} at the boundary is,

$$S_{\text{CT}} = -i\int d^4xC^\dagger Az^{1-2m}|_{z\to 0}, \tag{4.18}$$

giving the holographic renormalized action as,

$$S^{ren}_{\text{gravity}} = S_{\text{bdry}} + S_{\text{CT}}$$
$$= i\int d^4xD^\dagger A. \tag{4.19}$$

Picking up (4.19) with (4.3) and (4.5), the correlation function satisfies

$$D = -G_R A, \tag{4.20}$$

in the Weyl representation. This is not surprising since the boundary value ψ_0 of ψ is in fact a chiral spinor. On the other hand, the correlation function in the 2×2 matrix must be able to be written as the combination of the Pauli matrices as,

$$G_R = \alpha + \beta k_i\sigma^i, \tag{4.21}$$

we can set that the momentum is along the x^3 direction as $k_\mu = (-\omega, 0, 0, \text{k})$ due to the rotational symmetry in $\mathbb{R}^3 = \{x^i\}$, so that the correlation function G_R is expected to be diagonal, as

$$G_R = \begin{pmatrix}G^{1,1}_R & 0\\ 0 & G^{2,2}_R\end{pmatrix}. \tag{4.22}$$

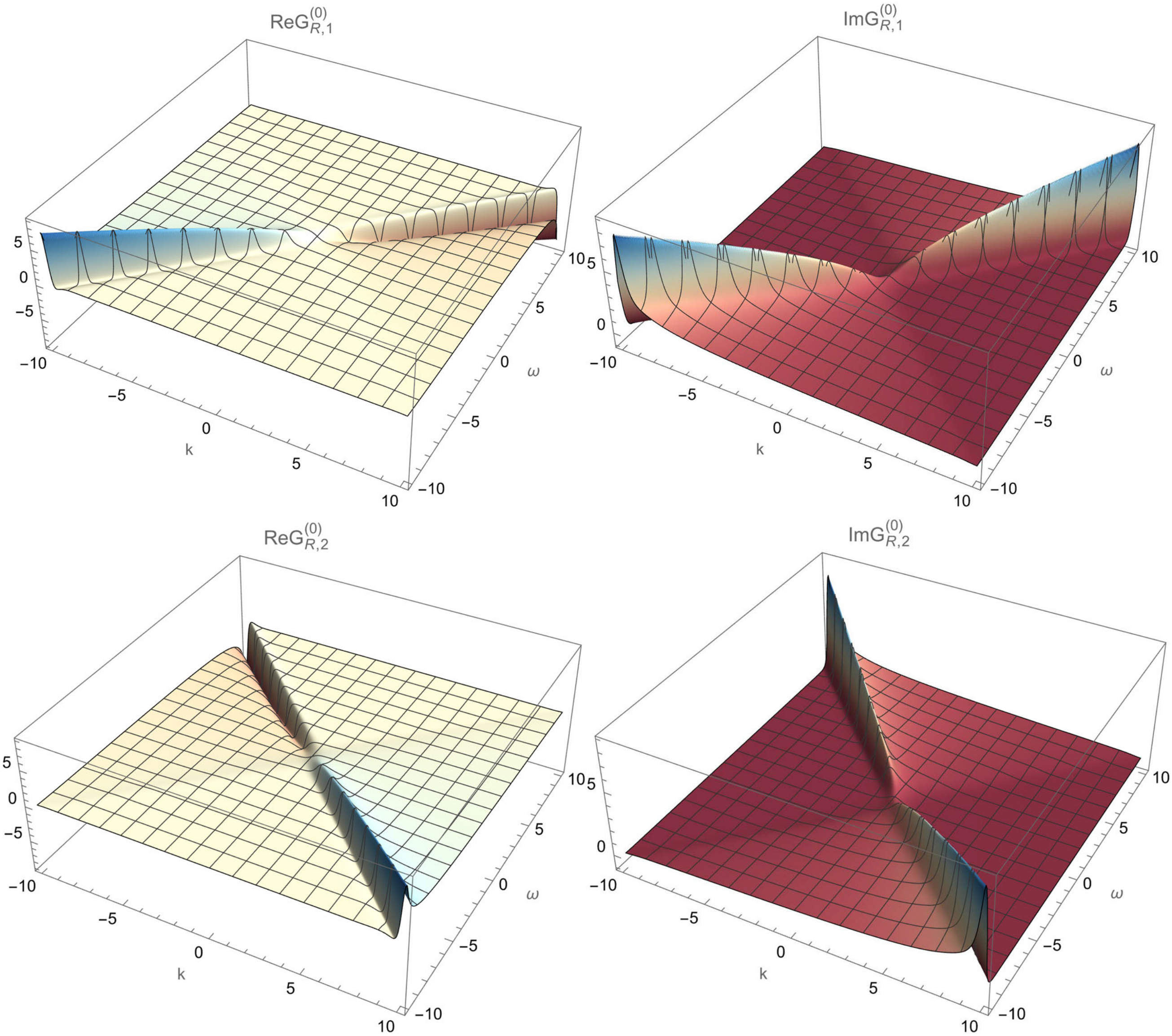

Fig. 2 The real and imaginary parts of zero-th order correlation functions $G^{(0)}_{R,\alpha}$ as functions of ω, k in the deconfined phase. The parameter is chosen as $q = 0, m = 0.01, z_H = 1$

To finalize this section, we introduce the ratio defined as

$$G_\alpha = (-1)^{\alpha+1} \frac{\chi_R^{(\alpha)}}{\chi_L^{(\alpha)}},\ \alpha = 1, 2. \tag{4.23}$$

According to (4.15)–(4.20), the correlation function is given by

$$G_R^{\alpha,\alpha} = (-1)^\alpha \lim_{z\to 0} z^{-2m} G_\alpha, \tag{4.24}$$

and the equations for the ratios can be obtained by recombining the components of the spinor χ with respect to the Dirac equation (4.11). As a result, one can find the equations for the ratios are given as,

$$\sqrt{\frac{g_{xx}}{g_{zz}}} G'_\alpha = (-1)^\alpha u - \mathrm{k} + \left[\mathrm{k} + (-1)^\alpha u\right] G_\alpha^2 + 2m\sqrt{g_{xx}} G_\alpha, \tag{4.25}$$

where "′" refers to the derivative with respect to z, and

$$u = \omega\sqrt{-\frac{g_{xx}}{g_{tt}}} = \frac{\omega}{\sqrt{f}}. \tag{4.26}$$

Therefore the correlation function could be evaluated numerically by solving (4.25) with the infalling boundary condition

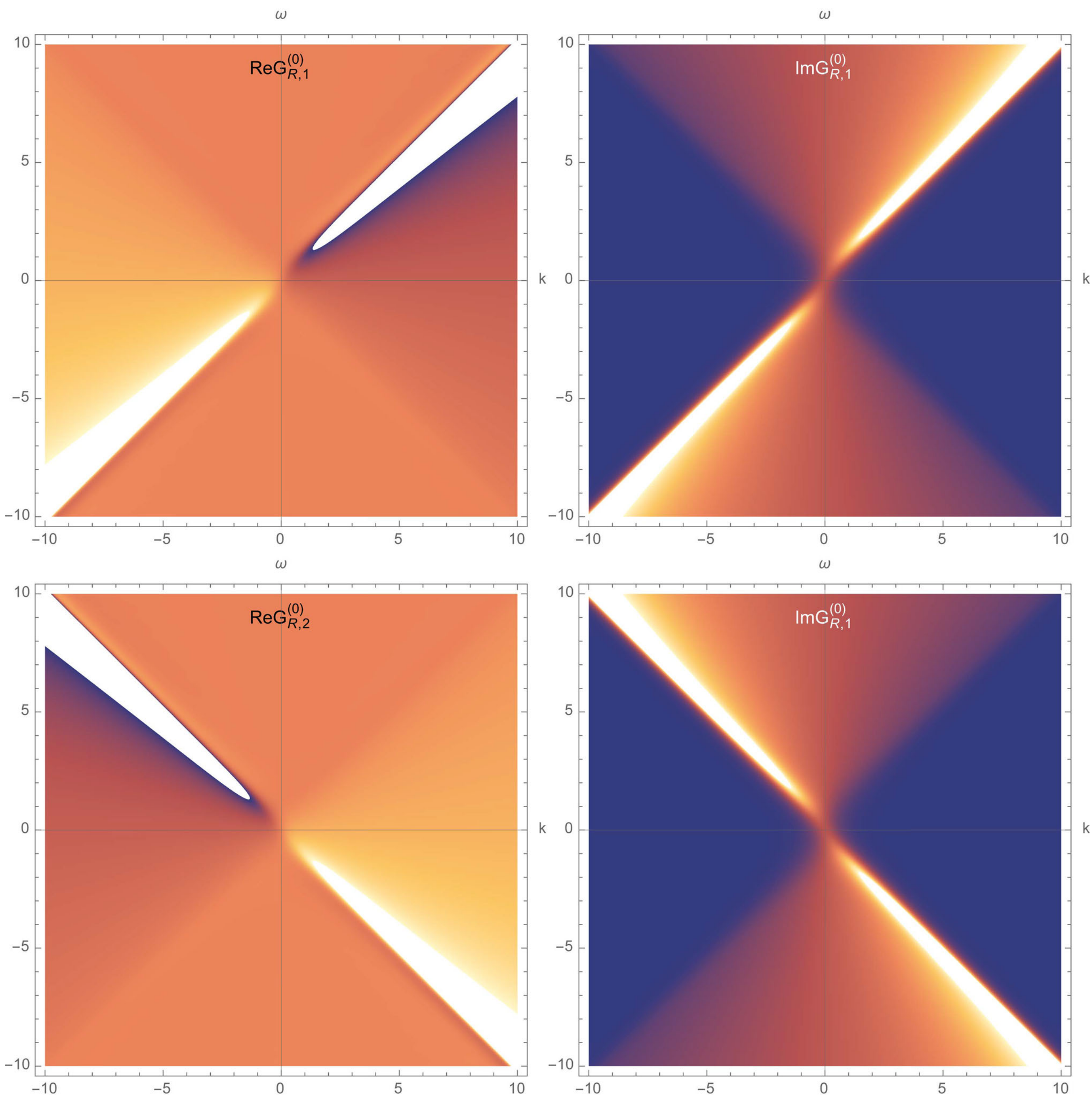

Fig. 3 Density plots of the zero-th order correlation functions $G^{(0)}_{R,\alpha}$ in the deconfined phase with the parameters as $q = 0, m = 0.01, z_H = 1$. The white regions refer to the peaks in the correlation functions

$G_\alpha|_{z=z_H} = (-1)^\alpha i$ obtained by analyzing its asymptotic behavior near $z = z_H$ as [35,42,46–48].

4.4 The numerical analysis

Deconfined phase

When the D-instanton is taken into account, the correlation function given in (4.24) should also depend on the charge density of the D-instanton denoted by q. In order to evaluate exactly the q-dependence in the correlation function, for $q \ll 1$ we consider its leading order correction by expand G_α as,

$$G_\alpha = \mathcal{G}_\alpha + q\xi_\alpha, \tag{4.27}$$

where $\mathcal{G}_\alpha$ is the zero-th order solution satisfying the equations presented in (4.25) with $q = 0$ as (there is no sum for the repetitive indices),

$$\sqrt{f}\mathcal{G}_\alpha' = (-1)^\alpha u - \mathrm{k} + \left[\mathrm{k} + (-1)^\alpha u\right]\mathcal{G}_\alpha^2 + \frac{2mR}{z}\mathcal{G}_\alpha. \quad (4.28)$$

Here we have inserted the deconfined geometry (2.10) into (4.25), and ξ_α is the leading order correction satisfying the equations

$$\sqrt{f}\xi_\alpha' = \left[\mathrm{k} + (-1)^\alpha u\right] 2\mathcal{G}_\alpha\xi_\alpha + \frac{2mR}{z}\left[\xi_\alpha - \frac{1}{4}\mathcal{G}_\alpha \ln f\right]. \quad (4.29)$$

By analyzing the asymptotic behavior of (4.28), we find the infalling boundary condition for $\mathcal{G}_\alpha$ could be $\mathcal{G}_\alpha|_{z=z_H} = (-1)^\alpha i$ which is exactly same as the infalling boundary condition for G_α. Therefore, the boundary condition for ξ_α is expected to be $\xi_\alpha|_{z=z_H} = 0$. Altogether, we will solve (4.28) and (4.29) numerically in order to evaluate the associated correlation function G_R as the fermionic spectral function in holography. We write down the correlation functions presented in (4.24) as the combinations of its zero-th order $G_{R,\alpha}^{(0)}$ and first order solution $G_{R,\alpha}^{(1)}$ as,

$$\begin{aligned} G_R^{\alpha,\alpha} &= G_{R,\alpha}^{(0)} + qG_{R,\alpha}^{(1)}, \\ G_{R,\alpha}^{(0)} &= (-1)^\alpha \lim_{z\to 0} z^{-2m}\mathcal{G}_\alpha, \\ G_{R,\alpha}^{(1)} &= (-1)^\alpha \lim_{z\to 0} z^{-2m}\xi_\alpha, \end{aligned} \quad (4.30)$$

where $\mathcal{G}_\alpha, \xi_\alpha$ are coefficients independent on q and they can be solved numerically through the equations (4.28) and (4.29). The corresponding numerical results for $\mathcal{G}_\alpha, \xi_\alpha$ are given in Figs. 2, 3, 4, 5 and 6.

Let us compare our numerical results with the calculations by using the method of hard thermal loop (HTL) in thermal QCD. The approach of HTL with vanishing chemical potential illustrates the dispersion curves of fermions (plasmino) is[5] [52,53],

$$\begin{aligned} &\omega(\mathrm{k}) \simeq m_f \pm \frac{1}{3}\mathrm{k} + \frac{1}{3m_f}\mathrm{k}^2,\ \mathrm{k} \ll 1; \\ &\omega(\mathrm{k}) \simeq \mathrm{k},\ \mathrm{k} \gg 1, \end{aligned} \quad (4.31)$$

where m_f is the effective mass generated by the medium effect of fermion as,

$$m_f = \sqrt{\frac{C_F}{8}}g_{\mathrm{YM}}T. \quad (4.32)$$

[5] We pick up the modes of positive frequency with $\omega > 0$ and momentum $\mathrm{k} > 0$, the case for the negative frequency can be obtained by replacing $\omega \to -\omega$.

Here g_{YM} refers to the Yang–Mills coupling constant and C_F is a constant suggested to be $C_F = 4/3$ for fundamental quarks or $C_F = 1$ for the electron. Accordingly, we can see the dispersion curves presented in the zero-th order correlation function given in Figs. 2 and 3 cover basically the behavior of dispersion curves from HTL at large momentum. For the small momentum, while the zero-th order dispersion curves may be close to the relation given in Fig. 6, it does not illustrate two branches of the dispersion curves as some related works in holography [35,42,46–48]. The reason may be that, according to the gravity/fluid correspondence [54,55], the plasma described holographically by the metric (2.9) with $q = 0$ corresponds to the conformally ideal fluid of $\mathcal{N} = 4$ super Yang–Mills theory which is different from the QED or QCD plasma. In particular, the interaction of the plasmino or the dissipation of the medium is not taken into account in the ideal fluid. While this issue may be expected to be figured out by taking into account the dissipation of the fluid somehow in the holographic background (2.9), we will focus on the influence on the instanton in this work.

For the case $q > 0$, the correlation function has a correction term $G_{R,\alpha}^{(1)}$ given by ξ_α as it is illustrated in Figs. 4, 5 and 6. For $\omega > 0$ and $\mathrm{k} > 0$, it is clear to see that the dispersion curves have two branches at small momentum and they trend to merge for large momentum. By taking a look at the value of the correction terms, we can find the correction $G_{R,\alpha}^{(1)}$ is large/small for small/large momentum respectively which has an opposite behavior to the zero-th correlation function $G_{R,\alpha}^{(0)}$. Altogether, for $q > 0$, the first order correction $G_{R,\alpha}^{(1)}$ dominates the behavior of the dispersion curves at small momentum and it always manifests two branches. At large momentum, the zero-th order function $G_{R,\alpha}^{(0)}$ dominates the behavior of the dispersion curves which displays only one branch of the dispersion curves on the light-cone. Therefore, the dispersion curves given by the total spectral function $G_R^{\alpha,\alpha}$ are very close to the relation for HTL (4.31).

Besides, our numerical results also illustrate that, i.e. for $\omega, \mathrm{k} > 0$, the effective mass $m_f = \omega(\mathrm{k} = 0)$ splits into two values as it is displayed in Fig. 5. This may be related remarkably to the properties of the fermionic spin, since it is known that there is spin-dependent interactions among fermions induced by instantons in QCD [1,2]. According to the calculations by one-gluon exchange, the massive quark potential depends on the quantum number of spin in the presence of instanton, so the total mass of the plasmino including quark interaction splits into two values which leads to two branches in the dispersion. In this sense, our numerical evaluation might be a holographic reproduction of the instanton-induced interaction with spin. However, for the massless case, the spin-dependent interaction induced by instantons trend to vanish, so it could be why the spectral function of massless fermion is not affected by the instan-

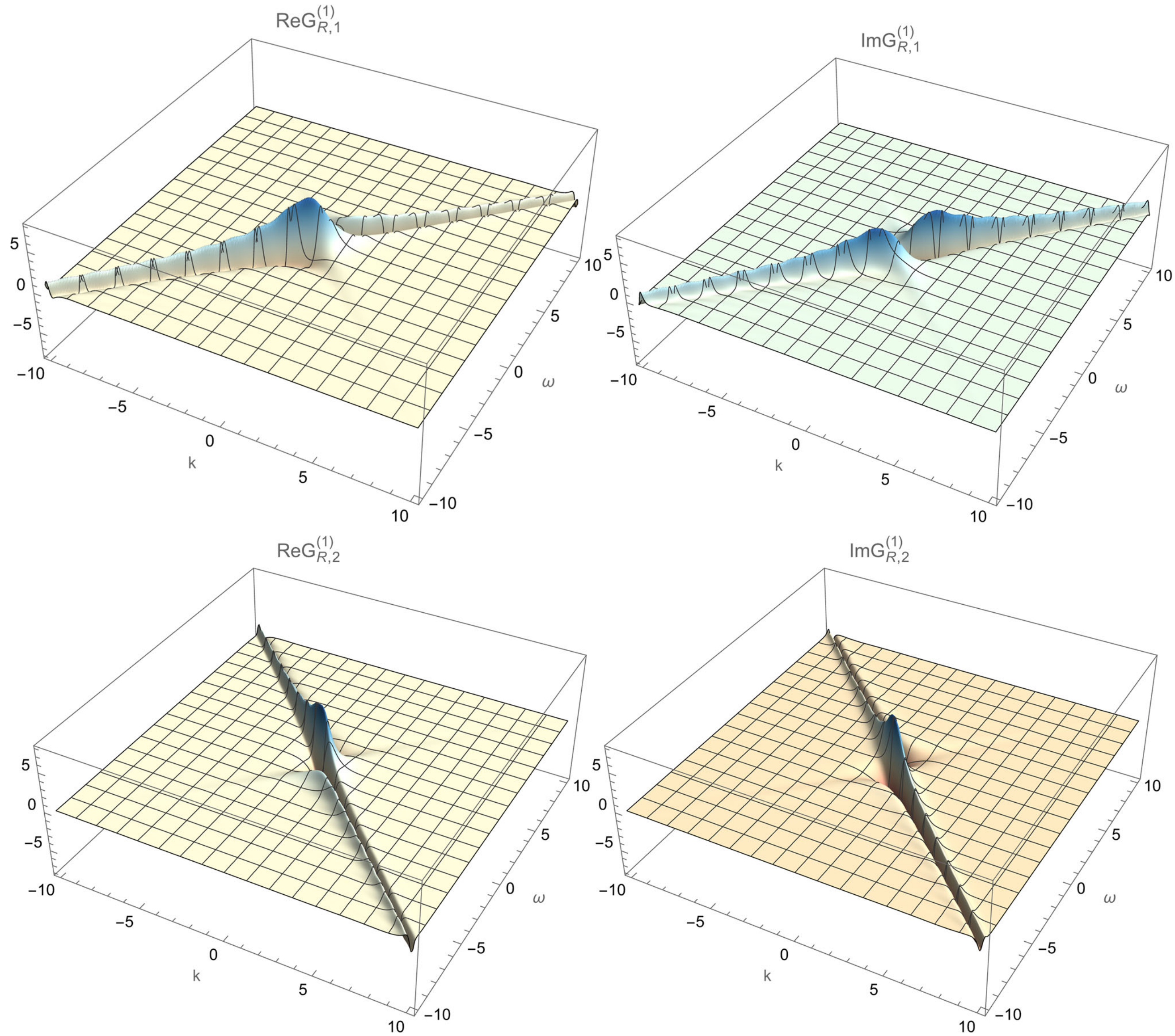

Fig. 4 The real and imaginary parts of leading order deconfined correlation functions $G^{(1)}_{R,\alpha}$ as functions of ω, k with $m = 0.01$, $z_H = 1$

ton charge. On the other hand, some existing works about D-instanton in gauge-gravity duality [24,28–33,35,42] also support that the property of mass for a massless hadron in plasma is not affected by the instanton, which could thus be a holographic confirmation.

Confined phase

As a parallel method to investigate the fermionic spectrum, we also evaluate numerically the equations in (4.25) with respect to the confined geometry given in (2.11). So the associated correlation functions are illustrated in Figs. 7 and 8. Comparing the confined correlation functions with the mass spectrum given in Table 1 and Fig. 1, we can see several separated peaks in the correlation function. Since the two-point fermionic correlation function is proportional to $\left(\not{k} - m\right)^{-1}$, the peaks refer to the separated dispersion curves regarding the various onset masses. In the confined correlation function, the onset position of ω at $\mathrm{k} = 0$ agrees with the fermionic spectrum and it basically holds for nonzero q, therefore the holographic correlation function indicates consistent conclusion of the fermionic spectrum with the method used in Sect. 3.

5 Summary

In this work, we study the spectroscopy of baryonic fermion in the D(-1)-D3 brane system. The geometric background of this system given by IIB supergravity includes a black and a

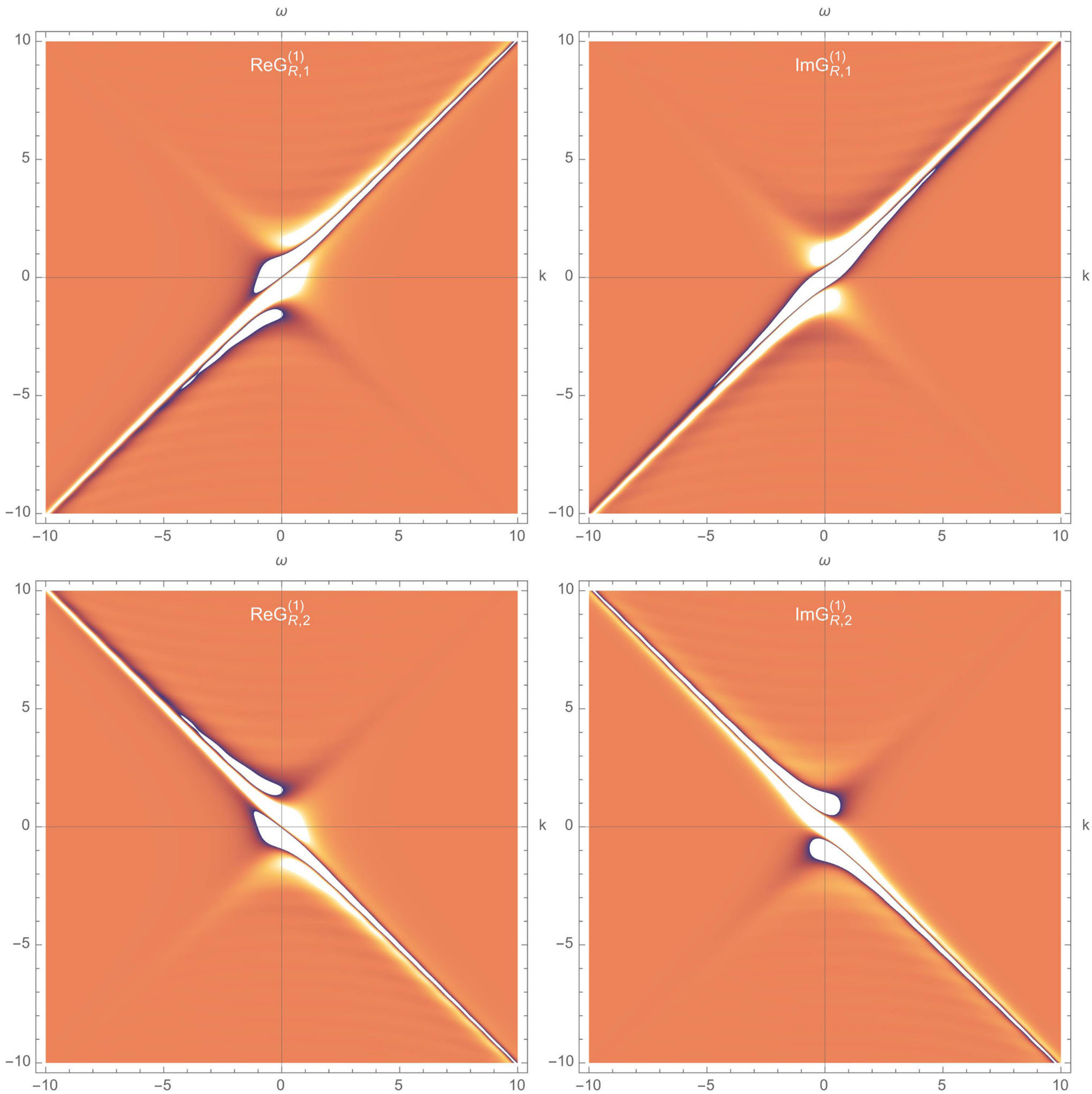

Fig. 5 Density plots of the leading order deconfined correlation functions $G^{(1)}_{R,\alpha}$ as functions of ω, k with $m = 0.01$, $z_H = 1$. The white regions refer to the peaks in the correlation functions

bubble solution which can describe respectively a deconfined and a confined gauge theory with instantons in holography. To simplify the setup, we briefly reduce the 10d supergravity background to an 5d background of gravity-dilaton-axion system. By considering a probe spinor in the 5d bulk, we illustrate the decomposition and dimensional reduction of the spinor, then obtain the fermionic spectrum in the confined geometry. Since the fermion must be a gauge-invariant operator according to the gauge-gravity duality, we further identify the fermion with a baryon in the confined geometry and compare our mass spectrum with the baryonic experimental data. However, as most works on holography [47,48], the gauge-invariant fermion in the deconfined phase is usually identified with the baryonic plasmino instead of the baryon since quarks and gluons can not form a baryon in the deconfined phase. Afterwards, we derive the equations for the holographic correlation function from the Dirac equation, then demonstrate the numerical calculations with the infalling boundary condi-

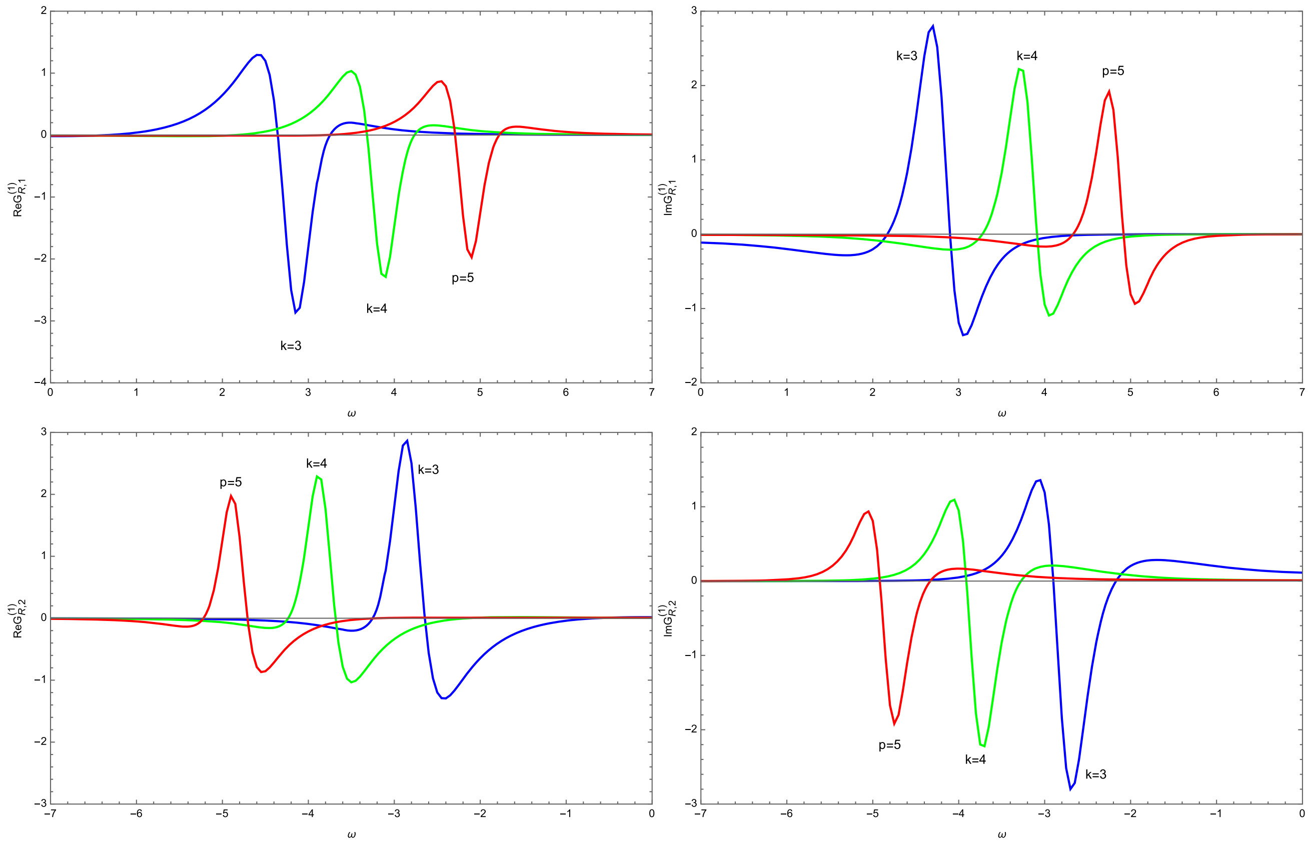

Fig. 6 The real and imaginary parts of leading order deconfined correlation functions $G^{(1)}_{R,\alpha}$ as functions of ω with various k and $m = 0.01$, $z_H = 1$. There are always two peaks for various k in the correlation function which correspond to the two branches of the dispersion curves

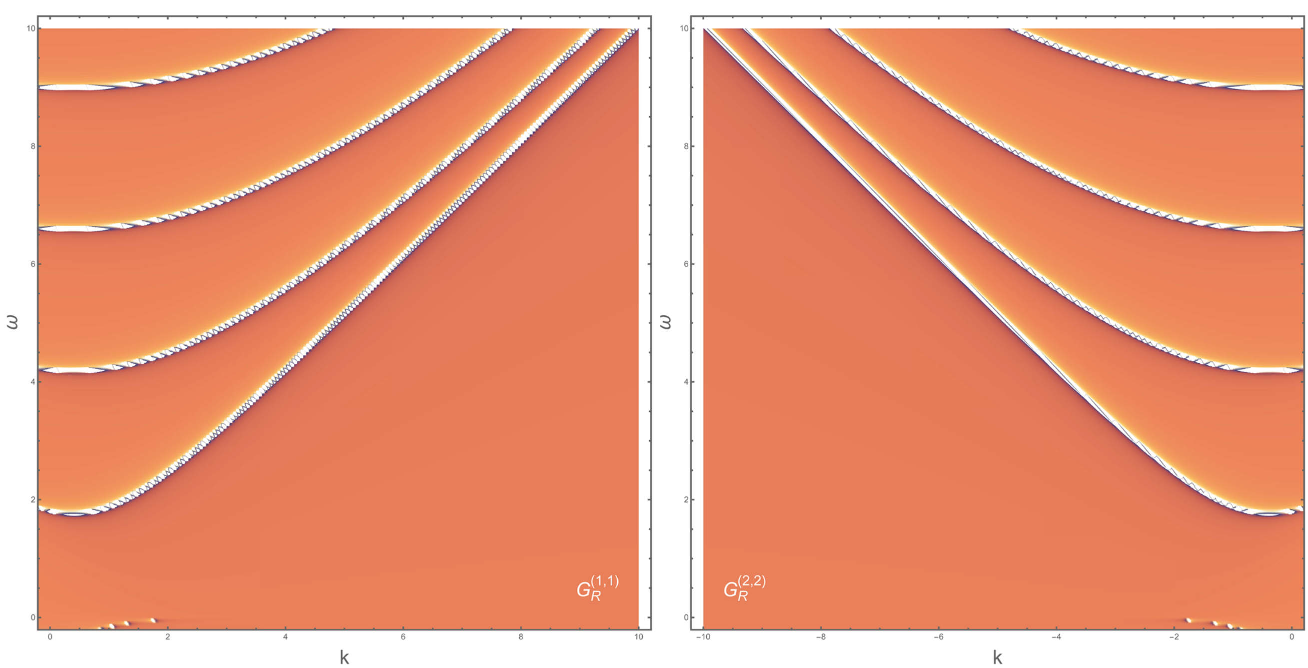

Fig. 7 The density plot of the holographic correlation function in confined phase with $q = 1$. The white region refers to the peaks in the correlation function

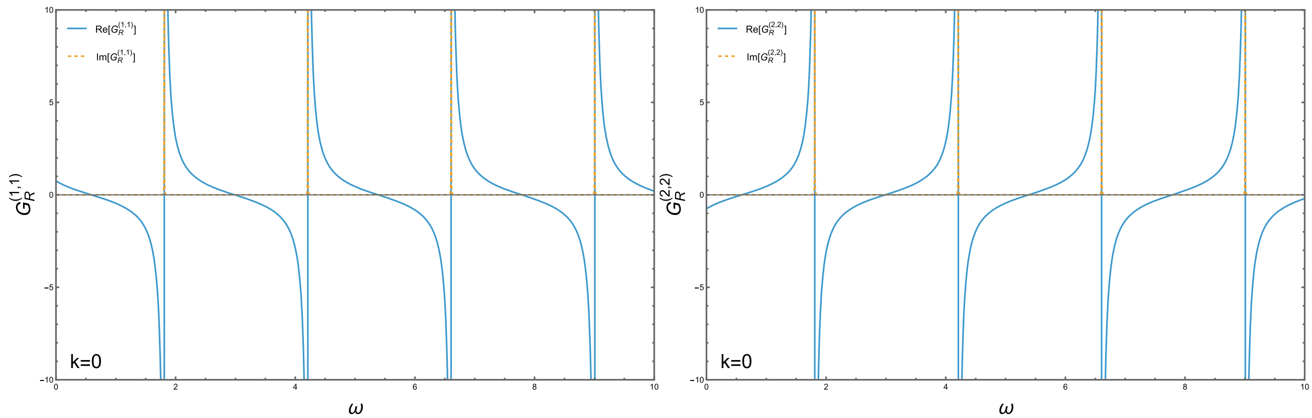

Fig. 8 The holographic correlation function as a function of ω at $k = 0$ in confined phase with $q = 1$

tion both in the deconfined and confined background. In particular, we expand the correlation function as zero-th order solution plus first order solution in the deconfined geometry. Our numerical results in the deconfined case illustrate that the first order correction to the total correlation function including two branches of the fermionic dispersion curves is dominated for small momentum, while the zero-th order correlation function dominates the behavior of the fermionic dispersion curves at large momentum giving only one merged dispersion curves on light-cone. This behavior is out of reach without the presence of the instanton and it is very close to the fermionic dispersion curves obtained by HTL. Furthermore, we also find the effective mass generated by the medium effect of fermion splits into two values which may be due to the spin-dependent interactions among fermions induced by instantons. Although it has be discussed qualitatively in the framework of QCD with instantons [1,2], it is interesting that the holographic approach reproduces this result. Besides, in the confined case, the holographic correlation function explicitly indicates that the position of the onset mass is consistent with the fermionic spectrum. Altogether, it means seemingly that the instantonic configuration in QCD is very influential on the spectroscopy of the fermion.

Acknowledgements We would like to thank Prof. Lin Shu for helpful discussion. This work is supported by the National Natural Science Foundation of China (NSFC) under Grant No. 12005033 and the Fundamental Research Funds for the Central Universities under Grant No. 3132025200.

Data Availability Statement This manuscript has no associated data. [Authors' comment: Data sharing not applicable to this article as no datasets were generated or analysed during the current study.]

Code Availability Statement This manuscript has no associated code/software. [Authors' comment: Code/Software sharing not applicable to this article as no code/software was generated or analysed during the current study.]

References

1. T. Schäfer, E. Shuryak, Instantons in QCD. Rev. Mod. Phys. **70**, 323–426 (1998). arXiv:hep-ph/9610451
2. D. Gross, R. Pisarski, L. Yaffe, QCD and instantons at finite temperature. Rev. Mod. Phys. **53**, 43 (1981)
3. E. Vicari, H. Panagopoulos, Theta dependence of SU(N) gauge theories in the presence of a topological term. Phys. Rep. **470**, 93–150 (2009). arXiv:0803.1593
4. D. Tong, TASI lectures on solitons: instantons, monopoles, vortices and kinks. arXiv:hep-th/0509216
5. D. Diakonov, N. Gromov, V. Petrov, S. Slizovskiy, Quantum weights of dyons and of instantons with nontrivial holonomy. Phys. Rev. D **70**, 036003 (2004). arXiv:hep-th/0404042
6. D. Diakonov, V. Petrov, Confining ensemble of dyons. Phys. Rev. D **76**, 056001 (2007). arXiv:0704.3181
7. Y. Liu, E. Shuryak, I. Zahed, Confining dyon-antidyon Coulomb liquid model. I. Phys. Rev. D **92**(8), 085006 (2015). arXiv:1503.03058
8. Y. Liu, E. Shuryak, I. Zahed, Light quarks in the screened dyon-antidyon Coulomb liquid model. II. Phys. Rev. D **92**(8), 085007 (2015). arXiv:1503.09148
9. Y. Liu, E. Shuryak, I. Zahed, The instanton-dyon liquid model III: finite chemical potential. Phys. Rev. D **94**(10), 105011 (2016). arXiv:1606.07009
10. Y. Liu, E. Shuryak, I. Zahed, Light adjoint quarks in the instanton-dyon liquid model IV. Phys. Rev. D **94**(10), 105012 (2016)
11. Y. Liu, E. Shuryak, I. Zahed, The instanton-dyon liquid model V: twisted light quarks. Phys. Rev. D **94**(10), 105013 (2016). arXiv:1606.02996

12. E. Poppitz, T. Schäfer, M. Unsal, Continuity, deconfinement, and (super) Yang–Mills theory. JHEP **10**, 115 (2012). arXiv:1205.0290
13. E. Poppitz, T. Schäfer, M. Ünsal, Universal mechanism of (semi-classical) deconfinement and theta-dependence for all simple groups. JHEP **03**, 087 (2013). arXiv:1212.1238
14. J. Maldacena, The large N limit of superconformal field theories and supergravity. Adv. Theor. Math. Phys. **2**, 231–252 (1998). arXiv:hep-th/9711200
15. O. Aharony, S. Gubser, J. Maldacena, H. Ooguri, Y. Oz, Large N field theories, string theory and gravity. Phys. Rep. **323**, 183–386 (2000). arXiv:hep-th/9905111
16. E. Witten, Anti-de Sitter space and holography. Adv. Theor. Math. Phys. **2**, 253–291 (1998). arXiv:hep-th/9802150
17. H. Liu, A. Tseytlin, D3-brane D instanton configuration and N = 4 superYM theory in constant selfdual background. Nucl. Phys. B **553**, 231–249 (1999). arXiv:hep-th/9903091
18. J. Barbon, A. Pasquinucci, Aspects of instanton dynamics in AdS/CFT duality. Phys. Lett. B **458**, 288–296 (1999). arXiv:hep-th/9904190
19. L. Bartolini, F. Bigazzi, S. Bolognesi, A. Cotrone, A. Manenti, Theta dependence in holographic QCD. JHEP **02**, 029 (2017). arXiv:1611.00048
20. S. Seki, S. Sin, A new model of holographic QCD and chiral condensate in dense matter. JHEP **10**, 223 (2013). arXiv:1304.7097
21. C. Wu, Z. Xiao, D. Zhou, Sakai-Sugimoto model in D0–D4 background. Phys. Rev. D **88**(2), 026016 (2013)
22. S. Li, A holographic description of theta-dependent Yang–Mills theory at finite temperature. Chin. Phys. C **44**(1), 013103 (2020). arXiv:1907.10277
23. S. Li, T. Jia, Matrix model and holographic baryons in the D0–D4 background. Phys. Rev. D **92**(4), 046007 (2015). arXiv:1506.00068
24. S. Li, Holographic heavy-baryons in the Witten–Sakai–Sugimoto model with the D0–D4 background. Phys. Rev. D **96**(10), 106018 (2017). arXiv:1707.06439
25. S. Li, S. Lin, D-instantons in real time dynamics. Phys. Rev. D **98**(6), 066002 (2018). arXiv:1711.06365
26. S. Li, S. Luo, M. Tan, Three-dimensional Yang–Mills–Chern–Simons theory from a D3-brane background with D-instantons. Phys. Rev. D **104**(6), 066008 (2021). arXiv:2106.04038
27. R. Argurio, A. Armoni, M. Bertolini, F. Mignosa, P. Niro, Vacuum structure of large *N* QCD_3 from holography. JHEP **07**, 134 (2020). arXiv:2006.01755
28. B. Gwak, M. Kim, B. Lee, Y. Seo, S. Sin, Holographic D instanton liquid and chiral transition. Phys. Rev. D **86**, 026010 (2012). arXiv:1203.4883
29. Z. Zhang, D. Hou, G. Chen, Heavy quark potential and jet quenching parameter in a D-instanton background. Eur. Phys. J. A **52**(12), 357 (2016). arXiv:1607.03985
30. Z. Zhang, D. Hou, G. Chen, Imaginary potential of moving quarkonia in a D-instanton background. J. Phys. G **44**(11), 115001 (2017). arXiv:1710.06579
31. J. Chen, D. Hou, Heavy quark potential and jet quenching parameter in a rotating D-instanton background. Eur. Phys. J. C **84**(4), 447 (2024). arXiv:2202.00888
32. S. Li, Holographic Schwinger effect in the confining background with D-instanton. Eur. Phys. J. C **81**(9), 797 (2021). arXiv:2005.11955
33. L. Shahkarami, M. Dehghani, P. Dehghani, Holographic Schwinger effect in a D-instanton background. Phys. Rev. D **97**(4), 046013 (2018). arXiv:1511.07986
34. W. Cai, K. Li, S. Li, Electromagnetic instability and Schwinger effect in the Witten–Sakai–Sugimoto model with D0–D4 background. Eur. Phys. J. C **79**(11), 904 (2019). arXiv:1612.07087
35. S. Li, Y. Zhang, H. Li, Correlation function of flavored fermion in holographic QCD. Phys. Rev. D **109**(8), 086020 (2024). arXiv:2307.13357
36. K. Becker, M. Becker, J.H. Schwarz, *String Theory and M-theory, A Modern Introduction* (Cambridge University Press, Cambridge, 2007)
37. J. Casalderrey-Solana, H. Liu, D. Mateos, K. Rajagopal, U.A. Wiedemann, *Gauge/Gravity Duality, Hot QCD and Heavy Ion Collisions* (Cambridge University Press, Cambridge, 2011). arXiv:1101.0618
38. I. Kirsch, Spectroscopy of fermionic operators in AdS/CFT. JHEP **09**, 052 (2006). arXiv:hep-th/0607205
39. R. Abt, J. Erdmenger, N. Evans, K. Rigatos, Light composite fermions from holography. JHEP **11**, 160 (2019). arXiv:1907.09489
40. T. Nakas, K. Rigatos, Fermions and baryons as open-string states from brane junctions. JHEP **12**, 157 (2020). arXiv:2010.00025
41. E. Witten, Baryons and branes in anti-de Sitter space. JHEP **07**, 006 (1998). arXiv:hep-th/9805112
42. S. Li, H. Li, Y. Zhang, Worldvolume fermions as baryons in holographic quantum chromodynamics with instantons. Commun. Theor. Phys. **77**(1), 015203 (2025). arXiv:2402.01197
43. S. Li, X. Zhang, Worldvolume fermion as baryon with homogeneous instantons in holographic QCD3. arXiv:2503.24173
44. M. Henningson, K. Sfetsos, Spinors and the AdS/CFT correspondence. Phys. Lett. B **431**, 63–68 (1998). arXiv:hep-th/9803251
45. W. Mueck, K. Viswanathan, Conformal field theory correlators from classical field theory on anti-de Sitter space. 2. Vector and spinor fields. Phys. Rev. D **58**, 106006 (1998). arXiv:hep-th/9805145
46. H. Liu, J. McGreevy, D. Vegh, Non-Fermi liquids from holography. Phys. Rev. D **83**, 065029 (2011). arXiv:0903.2477
47. Y. Seo, S. Sin, Y. Zhou, Thermal mass and plasmino for strongly interacting fermions. JHEP **06**, 076 (2013). arXiv:1305.1446
48. Y. Seo, S. Sin, Y. Zhou, Self-energy of strongly interacting fermions in medium: a holographic approach. Phys. Lett. B **723**, 207–212 (2013). arXiv:1205.3377
49. L. Fang, X. Ge, J. Wu, H. Leng, Anisotropic Fermi surface from holography. Phys. Rev. D **91**(12), 126009 (2015). arXiv:1409.6062
50. E. Witten, Anti-de Sitter space, thermal phase transition, and confinement in gauge theories. Adv. Theor. Math. Phys. **2**, 505–532 (1998). arXiv:hep-th/9803131
51. N. Iqbal, H. Liu, Real-time response in AdS/CFT with application to spinors. Fortsch. Phys. **57**, 367–384 (2009). arXiv:0903.2596
52. V. Klimov, Spectrum of elementary fermi excitations in quark gluon plasma. Sov. J. Nucl. Phys. **33**, 934–935 (1981)
53. V. Klimov, Spectrum of elementary fermi excitations in quark gluon plasma. Yad. Fiz. **33**, 1734–1736 (1981)
54. S. Bhattacharyya, V. Hubeny, S. Minwalla, M. Rangamani, Nonlinear fluid dynamics from gravity. JHEP **02**, 045 (2008). arXiv:0712.2456
55. S. Bhattacharyya, R. Loganayagam, S. Minwalla, S. Nampuri, S. Trivedi, S. Wadia, Forced fluid dynamics from gravity. JHEP **02**, 018 (2009). arXiv:0806.0006